NATIONAL ADVISORY COMMITTEE FOR AERONAUTICS

TECHNICAL MEMORANDUM

No. 1139

PLANING OF WATERCRAFT

By Herbert Wagner

TRANSLATION

"Jahrbuch der Schiffbautechnik," vol. 34, 1933

Washington

April 1948

NATIONAL ADVISORY COMMITTEE FOR AERONAUTICS

TECHNICAL MEMORANDUM NO. 1139

PLANING OF WATERCRAFT[1]

By Herbert Wagner

SUMMARY

Since form drag due to friction is nonexistent during gliding (or planing), the frictional drag can be applied as subsequent correction. The possibility of applying the conventional drag laws has already been partly verified by model test (Sottorf). These frictional forces are not discussed further.

Infinitely small inclination of the bottom in a frictionless fluid, the drag can be separated exactly into wave drag and spray drag: wave drag contains the total motion energy remaining behind the planing surface; when infinitely thin spray hits the water surface, the energy contained in it is dissipated as turbulence. Further division of the wave drag at low speeds into a gravity effect (displacement drag) and a dynamic effect (planing drag) does not appear possible forthwith. At high speeds, or more accurately, for great wave lengths compared to planing surface dimensions, the motion energy (wave energy) remaining behind the planing surface becomes independent of gravity; hence it is identical with the induced drag of the gravity-free motion.

At great (finite) angles of attack an exact division of the drag into wave drag and spray drag is not possible.[2] The water pushed downward behind the planing surface and the water from the sides meet and throw up new sprays, and the air carried deep down below the water surface itself is indicative of the formation of vortex surfaces and its correlated energy dissipation. At low speeds the water flowing laterally strikes the rear portion of the sides of the planing boat and shoots up into the air.

---

[1]"Über das Gleiten von Wasserfahrzeugen." Jahrbuch der Schiffbautechnik, vol. 34, 1933, pp. 205-227.

[2]The decomposition of the ship drag into friction drag, form drag, and wave drag is, after all, only a technical expedient.

The processes during rapid planing and at small angles of attack including nonstationary motion appear to be theoretically explained by the airfoil comparison. In some simple cases of rapid planing exact information is obtainable by the theory even for finite inclination of planing bottom.

However, it should be borne in mind that the attitude of slow planing is technically important also and accurate information regarding it is still very scarce.

INTRODUCTION

The present report deals with the processes accompanying the planing of a planing boat or a seaplane on water. The study is largely based upon theoretical investigations; mathematical problems and proofs are not discussed. To analyze theoretically actual planing processes, giving due consideration to all aspects of the problem, is probably not possible. The theories therefore treat various simple limiting cases, which in their entirety give a picture of the planing processes and enable the interpretation of the experimental results. The discussion is concerned with the stationary planing attitude: the boat planes at a constant speed V on an originally smooth surface.

Limiting Case of Rapid Planing, that is, Gravity Disregarded

The discussion starts with the condition of very fast planing of a small boat. The faster the boat planes the greater the dynamic forces (planing forces), and the greater the reduction in the static pressure of the water (displacement lift) relative to these forces. The order of magnitude is given by the depth of immersion of the boat (references 1 and 2). This ultimately leads to disregarding the static pressure; that is, it leads to the concept that the fluid with the originally flat, free surface is in a space devoid of gravity.

Flat Plate, Two-Dimensional Problem (Reference 2)

The simplest form of the planing bottom is a flat plate with very great (infinite) width. Figure 1 shows the form of the free surface and pressure distribution for different angles of attack β; spray is thrown forward. The speed of the water in the spray (for a moving planing surface) is almost twice as great as the planing speed V.

The planing force R can be computed; it acts perpendicular to the plate. Energy is needed to overcome the drag $W = R \sin \beta$. Behind the

planing surface the water eventually becomes perfectly still; hence no energy remains. The entire energy corresponding to the drag W is dissipated in the spray. Only spray drag, that is, drag corresponding to the spray energy, occurs, and no wave drag. The same holds for gravity-free motion for infinitely wide planing surfaces of any profile.

At point C, where the flow divides, the highest pressure at all angles of attack is the dynamic pressure $p_{max} = \frac{1}{2} \rho V^2$. At small angles of attack the pressure in the entire rear portion of the plate drops linearly with decreasing angle of attack; at infinitely small angle of attack it is infinitely small compared to the pressure peak at the forward edge. This small area at the forward edge is termed the spray root. This flow area is, at small angles of attack, geometrically similar for all angles, its measure is defined by the spray thickness δ. Since this thickness, like the drag, decreases proportionally with the square of the angle of attack, the area of the spray root at very small angles of attack is extremely small, and almost pointlike. The region beyond the spray root is designated as the principal area.

The root area can be computed independently of the rest of the flow, (reference 2, p. 197). It is illustrated in figure 2.

Plates with Infinitely Small Angle of Attack

Airfoil Comparison (Reference 2, p. 199)

Figure 3 illustrates the flow past a flat wing of infinite span. The thickness of the wing is very (infinitely) small. The flow at the trailing edge is smooth, as for the planing surface. There is, however, at high speed an upward flow around the leading edge of the wing (fig. 3, bottom). Since a high negative pressure corresponds to a high speed, the leading edge of the wing is pulled forward by the fluid. The force introduced here is called the "suction force" S, and the flow in the area of the leading edge the "suction point." The rest of the flow area is designated as principal area. In this principal area the pressure is perpendicular to the flat plate. The positive pressure R on the lower surface is as great as the negative pressure R on the upper surface. The resultant 2R of this pressure is inclined to the rear. The resultant of S and 2R gives the total force T at the wing. Since, aside from fluid friction, a wing of infinite span experiences no drag, this resultant is perpendicular to the flow velocity V.

Now it can be proved that in the lower half of the principal area of the wing and in the principal area of an identically formed planing surface (cf. figs. 3 and 4) identical flows prevail, provided the angle of attack is infinitely small. The lower surface of the planing surface

then experiences the same force R as the lower surface of the wing. Suction force does not appear on the planing surface; in its place there occurs the spray. Therefore the total force R on a planing surface is equal to half the total force T of the identically formed and identically moving wing, less half the suction force S, or mathematically expressed: $R = \frac{1}{2} T + (-\frac{1}{2} S)$.

This comparison is valid for surfaces of any shape, any boundary, and any stationary or nonstationary motion, so long as the angles of inclination of the surfaces are everywhere very (infinitely) small and gravity can be disregarded. On the planing surface the suppression of the suction force of the wing corresponds to the foundation of the spray drag $W_S = \frac{1}{2} S$. The spray thickness is therefore defined by the suction force of the wing: $\delta = \frac{S}{4\rho b V^2}$. Suction flow of wing and root flow of the planing surface become identical toward the border of these areas and change smoothly into the principal flow. Figure 5 indicates the form of the surface for several infinitely wide, circular curved planing surfaces. Lift, drag (spray drag), and spray thickness are obtained from simple equations (cf. appendix). An upwardly curved plate with zero angle of attack gives a lift without experiencing drag. Downwardly curved plates experience either an upward or a downward force depending on the angle of attack. Downward camber lowers the lift and raises the spray drag as compared with the flat plate.

Application of Airfoil Comparison to Plate of Finite Span

A brief summary of the results of Prandtl's airfoil theory (reference 3) is indicated. In contra distinction to the wing of infinite span, for the wing with finite span b the fluid pressed downward by the wing can escape laterally upward and flow toward the upper surface (fig. 6). This additional downward velocity occurs in front of the wing, and has a magnitude

$$v_i = \frac{2T}{\pi \rho V b^2} \tag{1}$$

in the median area of the surface and increases to $2v_i$ far behind the wing. This downwash v_i is almost constant over the entire wing span. It is dependent upon the lift T and the plate width, but not on the shape. Thus, compared to the plate of infinite span the flow experiences a downward inclination for a downwash angle $\beta_i = v_i / V$ and, in addition a curvature.

Consider first the case of the wing that is short compared to its width (l smaller than about 1/3 b). In this instance for a good

approximation the curvature of the flow can be neglected; that is, the angle of downwash β_i may be considered constant in the entire range of the wing. Flow in the zone of the wing and forces then correspond to those of a wing with infinite span at an angle of downwash β_i, making $\beta_w = \beta - \beta_i$ the "effective angle of attack" of the wing with finite span. In consequence (cf. fig. 7), the force is inclined backward an amount β_i; the wing of finite span thus experiences a drag $W_i = T\beta_i$, called the "induced drag." This drag finds expression in the motion energy of the downwash remaining behind the wing.

This argument is now applied to the planing surface (cf. figs. 19, 20). The planing surface of finite width b and no excessive length is subjected to the same lift A and the same spray drag W as an identically wide piece of an infinitely wide plate of the same profile but set at an angle is less by

$$\beta_i = \frac{4A}{\pi \rho V^2 b^2} \tag{2}$$

To this is added, an induced drag due to downwash

$$W_i = \frac{4A^2}{\pi \rho V^2 b^2} \tag{3}$$

which is dependent upon the total lift and the width of the plate, but independent of the plate form, (hence of the pressure distribution over the plate). Since this drag corresponds to the motion energy in the water behind the planing surface, it is logically identical with the wave drag of a planing process under the effect of gravity.

For plates of great length (reference 4) it is necessary to consider, aside from the inclination of the flow, its curvature. The behavior of the flat plate in curved flow is exactly the same as that of a plate with downward curvature in a rectilinear flow (fig. 8), so that – with respect to the theory of the short plate and given angle of attack – the lift and hence the induced drag is decreased, but the spray drag is increased.

Figure 9 shows the induced drag and the spray drag compared to the total drag for flat planing surfaces. For very short plates the spray drag equals the total drag; it then decreases and reaches the minimum proportion of about 45 percent at around $l/b = 1.3$. For longer plates its proportion rises again and ultimately reaches 1/2 for very long plates. It is emphasized that this result holds exactly only for gravity-free motion and for very (infinitely) small angles of attack.

The induced drag is not avoidable for any given plate width. On the other hand, the spray drag can be minimized by appropriate design shape (curvature of plate), if this is consistent with the other properties of the planing boat.

V-Bottom Planing Surface

A slight V (fig. 10) affects the lifting force very little according to both the theory and the tests. Induced drag and spray drag are in the same ratio as for flat plates. Curvature of the planing bottom in the longitudinal direction lowers the spray drag in the same degree as for flat plates. (A very simple situation is obtained for the "extreme case of long planing surface," reference 2.)

The spray is projected laterally (cf. figs. 21, 22, 23). If the normal to the forward edge of the pressure surface is plotted in plan (fig. 12), the angle between the planing direction and the direction of velocity v_{rel} of the spray water relative to the boat is bisected (reference 2, p. 2, last paragraph). The magnitude of the relative velocity is V. The absolute velocity v_{ab} on boats with greater V and especially small angle of attack β, is very much smaller than the spray velocity 2V of boats with zero V-bottom. Since the sprays have the same energy, however, they are correspondingly thicker on the V-bottom boat.

The flow processes in the forward area can be approximately compared with the vertical penetration of a wedge into the fluid surface at a speed $V\beta$. The latter process yields to theoretical solution, as will be shown elsewhere (cf. fig. 17).

The ensuing pressure distribution is shown in figure 10. Some data is afforded by the theory regarding the decrease in planing force for marked V-bottom, but these uncertain results will not be discussed.

Effect of Friction

On the planing surface the speed increases from the stagnation point in direction of the flow, that is, forward and rearward, respectively, (fig. 11). In such cases, according to Prandtl's boundary layer theory, the viscosity of the fluid merely causes the appearance of a frictional force in the direction of the plate, which can be subsequently accounted for. Separation phenomena and vortex formations similar to the processes at the upper surface of a wing or at the stern of a ship, cannot occur on flat or slightly curved planing surfaces (on markedly curved plates with small angle of attack (fig. 5, top, for example) the speed along the flow can, of course, decrease); such planing surfaces have no form drag.

When considering the frictional force the friction of the spray thrown forward at the bottom must also be observed. At small angles of attack β the dynamic drag $W = R \tan \beta$ is low and accordingly the spray on flat-bottom planing surfaces is very thin. For the Sottorf model tests with planing surfaces the calculation gives spray thicknesses of from about 0.1 to 0.2 millimeter at 5° angle of attack. If the entire spray were exactly in forward direction and completely decelerated by the friction at the bottom the frictional force directed forward would be half as great as the spray drag. The spray, however, very likely hits the water before complete deceleration, and besides, part of the spray is directed obliquely sideways as a result of the curvature of the forward contour of the pressure area. In consequence only a portion of half the spray drag can be recovered by the friction.

On V-bottom boats (fig. 10) and even more so on planing boats with greater V or less angle of attack, the relative speed governing the friction, is inclined obliquely backward. Thus the spray drag is augmented by the backward directed frictional drag of the thick spray water layer.

Consideration of Gravity Effect

Because of the mathematical difficulties involved in comprehending the effect of gravity, knowledge concerning this condition is meager. The following considerations are given with the aid of the results of the gravity-free condition. Consider, first, the two-dimensional flow problem (fig. 12). A plate of very (infinitely) great width b is held in the flow. The plate then experiences a pressure p on its lower surface. It was, however, not possible to obtain a satisfactory explanation of the relations between pressure distribution and plate form. On the other hand, success (reference 5) in computing the drag of the plate for any chosen pressure distribution on the premise of infinitely small inclination of the fluid surface was obtained. The pressure area is divided into separate pressure lines with the lifting force $\Delta R = p\, b\, \Delta x$. Each pressure line produces, aside from a local disturbance, a wave emanating from it of height

$$\Delta a = \frac{2\Delta R}{\rho V^2 b} \tag{4}$$

The total wave behind the pressure surface consists of the sum of all these individual waves of the same wave length, however, the different origins (of the various pressure lines) must be noted. The height a of this total wave determines the wave energy and hence the wave drag (gravity drag) of the planing surface:

$$W_g = \frac{1}{4} g \rho a^2 b \tag{5}$$

Hence, if the length of the pressure surface (planing surface) is small relative to the length of a wave, that is, if all the individual waves emanate from almost the same place, the height a of the total wave

$$a = \frac{2R}{b \rho V^2} \tag{6}$$

is independent of the special pressure distribution and the eventual appearance of a pressure peak, that is, independent of the form (of the profile) of the planing surface. The wave drag also

$$W_g = \frac{1}{4} g \rho a^2 b = \frac{R^2 g}{\rho V^4 b} = \frac{2 \pi R^2}{\rho V^2 b L} \tag{7}$$

is independent of the profile of the planing surface.

The wave drag is proportional to the acceleration of gravity g; for gravity-free motion and infinite plate width there is no wave drag, in accord with the foregoing considerations. How does this drag-producing effect of gravity originate? [1]

In gravity-free motion the water in front of the pressure surface rises (fig. 13); this area is called "impact area." This rise is diminished through the action of gravity, or in other words, in comparison to the gravity-free motion the acceleration of gravity imparts a supplementary, downward velocity v_g to the water before the planing surface. If, for example, the pressure area is short compared to the length of the impact area, the downward velocity in the area of the pressure surface is very approximately constant. This corresponds to a rotation of the entire flow picture through an angle of $\beta_g = \frac{v_g}{V}$. Since the drag introduced by the gravity is already exactly known, β_g is computed from the relation (fig. 13)

$$\beta_g = \frac{W_g}{A} = \frac{R_g}{\rho V^4 b} \tag{8}$$

---

[1] (The following consideration merely serves to illustrate the process and, above all, to estimate the change in gravity effect on plates of finite width. That the gravity effect on infinitely short plates can be represented by a rotation of the flow picture according to equation (8) follows from the independence of the gravity effect on the pressure distribution. The proof can be adduced in similar manner as in the author's article, reference 2, par. 12).

For the sake of clearness the form of the pressure surface had been chosen so as to produce no spray. But if a flat plate is used, for example, there is a gravity drag $W_g = \beta_g R$ to which corresponds the rotation of the flow pattern through angle β_g and the wave energy, and in addition, the spray drag $W_s = (\beta - \beta_g) R$ corresponding to the spray.

The spray drops back in the water in front of the plate, where its energy is dissipated as turbulence. Because the theory of the pressure lines postulated infinitely small inclination of the fluid surface it has failed for all plate forms on which sprays originate (and this includes practically all the utilized plate forms), since the inclination of the fluid surface at the spray is nearly 180°. After grasping the relation it was easy to account for the spray on short plates. However, it is not difficult to apply the pressure line theory to such flow processes even for finite plate length (cf. appendix).

Finite Plate Width

An estimation will give a picture of the several effects for plates of finite width. First, consider again the plates of very small length. Spray and spray drag may be discounted for the present. It can be determined later for the given plate form when the downwash due to gravity and finite plate width is known.

The gravity drag for such a short plate is computed as in the case of an infinite plate width and the induced drag is computed separately for gravity-free motion, thus

$$W_g = \frac{2\pi}{L} \frac{R^2}{\rho V^2 b} \qquad W_i = \frac{4}{\pi b} \frac{R^2}{\rho V^2 b}$$

According to these formulas the gravity drag is smaller than the spray drag, when $b < \sim 1/5\ L$. But then it is also possible to compute for gravity-free motion the impact area for finite plate width (reference 2, par. 12), and this calculation shows that the volume and the forward extent of the impact area diminishes very rapidly with decreasing plate width. From this it can be concluded that the gravity drag introduced by the impact area is substantially less on plates of finite width than for plates of infinite width, so that for plates of $b < 1/5\ L$ this effect of the gravity should be unimportant. Hence for this range of small plate widths which comprises the technically important processes, the induced drag comes close to the correct value.

Expressed in other words: while the water is pressed downward behind the plate and laterally upward behind the plate of finite width

(fig. 6), and gives rise to a wave motion due to the action of gravity, these processes behind the short plate have no rectroactive effect on the flow at the plate. The wave drag (if one wants to call it that) is identical with the induced drag. If the narrow plate is long its after-part falls into the region of upward velocity produced by gravity. The drag (wave drag) is then, as the tests also indicated, smaller than the induced drag for gravity-free motion, the gravity then has a drag-reducing effect.

An attempt is made to obtain an understanding of the region of transition from floating to planing by means of a calculation. (Compare the test data for the speed of maximum water drag of hydroplanes, Schiffbau, July 1929). A flat planing surface with vertical side walls at rest has the displacement lift $A_{depl} = 1/2\,\gamma\, b\, l^2\, \beta$, a surface gliding over gravity-free fluid has the planing lift according to equation (19) (with $f = 0$). The two formulas yield identically great lift values, when

$$l = \frac{L}{2\left(2 + \frac{l}{b}\right)} \tag{9}$$

hence, for example:

for $\frac{b}{l} = \infty$, when $\frac{l}{L} = \frac{1}{4}$

for $\frac{b}{l} = 1$ when $\frac{l}{L} = \frac{1}{6}$

for $\frac{b}{l} = \frac{1}{3}$ when $\frac{l}{L} = \frac{1}{10}$

It is estimated that the transition in these conditions of plate length and wave length takes place between the predominance static lift and the planing attitude.

Comparison with Experiments

For gravity-free motion, the planing force R, in otherwise identical conditions, increases proportionally to v^2. The value R/v^2 is therefore, at given plate width, dependent only upon the angle of attack β and length l of the pressure surface. Figure 14 shows β plotted against l for four R/v^2 values with plates of 30-centimeter width according to Sottorf's planing tests (reference 6). The tests were

made at four speeds; the test points for the same speed are combined into a curve. The curve computed for gravity-free motion by the short plate theory is also shown.

In the two top figures (and also approximately in the third) the test series with the high speeds $V = 6.8$ and 9.5 meters per second coincide. Since the Froude number and consequently gravity has no influence, in these tests an exact theory of gravity-free motion should agree with these tests. For the short lengths, and particularly under the small loading, (top fig.), that is, at small β compared to the other figures, the test curves are up to 20 percent above the theoretical curve. Part of this discrepancy may be attributable to the fact that in the test the maximum length of the wetted surface, namely, the length in the center of the planing surface, was observed, while the theoretical curve refers to the mean length. Probably the effect of the friction on the thin spray itself has slightly modified the flow in the area of the forward edge with respect to the theory. The scattered test points for small lengths seem to point toward this effect.

For greater lengths ($l > b/2 = 15$ cm) and small β (top fig.) the short plate theory yields, as stated, too much lift and too small β. With some effort this divergence could also be determined theoretically.

For great l and great β, on the other hand, the water streams past the long side edge with laterally directed speed (fig. 15); in comparison to small β a wider portion of the fluid is pressed downward[1]; the angle of attack is then smaller than computed by theory. (Cf. figs. 3 and 4.) The same phenomenon occurs, although not as conspicuously, in airfoil tests (reference 4).

In the tests at low speed $V = 4$ meters per second the gravity has a substantial lift-increasing and drag-decreasing effect, especially at great lengths. Since in this case the wave length amounts to $L = 10$ meters, it closely approaches the length for the transition from floating to planing given by equation (9).

---

[1]It is suspected that a wider water mass entails a greater spray drag (similarly for planing of a wider plate). In agreement with this sprays appear to rise from the forward edge of the pressure surface as well as from the sides (from the tips of fig. 15). The absolute speed, however, and hence the energy in these sprays is probably small. A detailed discussion of these sprays seems superfluous, since a definite separation of spray drag and wave drag at finite angles of inclination of the plate is, moreover, not possible.

Pressure-Point Theory

This important zone of transition from floating to planing can be analyzed by the pressure point theory. As in the two-dimensional problem where the pressure surface was replaced by pressure lines, the action of a finite planing surface can be represented by a distribution of pressure points on the fluid surface. Calculation of the accompanying wave drag has actually been accomplished by Havelock and Hogner, and Weinblum worked out a number of model problems (reference 7).

However, this theory still offers some difficulties. First of all, success was not attained in computing the form of the planing surface for a given pressure distribution; hence, an analysis of the effect of the form on wave drag and particularly on spray drag should prove difficult. Furthermore, in the theory the finite pressure distribution is replaced by the Fourier integral theorem (infinite series of sine functions). This substitution, however, leads in the extreme case of an infinitely small planing surface, to an infinitely great error (of course, only logarithmically great); the calculation then gives too high a drag by an amount

$$\frac{16\,R^2}{\pi\,\rho\,V^2\,b^2}\ln\frac{bV^2}{gl^2}$$

This error prevents the tie-in with the gravity-free motion and makes a clear representation of the gravity effect difficult. Moreover, the transition from floating to planing does take place on planing surfaces of small dimensions compared to wave length, and it would have to be explained how great the error is in this zone. And lastly, allowance for the pressure peak as it consistently occurs at the forward edge, should result in an increase of the error, and so to an apparent increase in wave drag which does not exist at all in reality.

Weinblum's calculation indicates that the defects of the theory, for small planing surface, are in the expected direction; but the drag-reducing gravity effect for long, narrow plates is also manifest. It is anticipated that the pressure point theory will ultimately succeed in giving a clear representation of the gravity effect for the case of small β.

Nonstationary Processes

Impact at a Step

Illustrative of a nonstationary process is the impact of a step (two-dimensional problem) for gravity-free motion shown in figure 16 (reference 2, p. 208). C is the point at which the step first touched the water. The arrows indicate the speed at several points of the surface. In the shaded area over the surface fairly high horizontal speeds prevail. The spray reaches up to D. The impact force can be calculated; the pressure distribution was not computed.

Impact of V-Bottom Boat

Figure 17 shows the vertical impact of a V-bottom boat (of infinite length) on the water (references 2, and 8), as represented by the drop of a planing boat tossed upward by the waves. The form of the water level and the pressure distribution for several successive phases of this process are indicated.

The reaction to the downward acceleration of the water is a pressure on the planing surface. Since in the subsequent course the mid-area of the water has already assumed the speed of the boat, and on the edge new parts of the water are involved, the pressure at the edge of the pressure surface is great, especially if the bottom surface has little inclination. Since the boat and hence the downward moving water is decelerated again during the process, negative pressures may even occur in the median part of the boat. The spray flung off laterally contains the greater part of the motion energy given off by the body on the water. Assuming a rigid boat the calculation is comparatively easy for any form of bottom.

Description of Photographs

Figures 19, 20, 21, and 23, are photographic records taken in the Hydraulics and Marine research laboratory. Figure 22 is taken from a report by Sottorf (reference 6).

Figure 19: flat, planing glass plate, photographed vertically from above; width $b = 20$ centimeters, length of pressure surface $l = 35$ centimeters, over all length of plate: 60 centimeters, angle $\beta = 10^{\circ}$; planing speed $V = 6.5$ meters per second.

In these and in the succeeding photographs the camera moved with the planing surface.

The spray thrown forward (calculated thickness about 0.8 mm) is retarded by the friction on the glass plate and ultimately stopped by the relative wind and bent back. Almost all of the spray comes from the front edge of the pressure surface, and the spray leaving the lateral points of the forward edges obliquely backward are plainly visible. Only a small amount of spray shoots from the side of the plate at the water surface (fig. 15), and its absolute speed is low, the apparently high speed (that is, the relative speed) is only due to the fact that the camera moves with it.

The disturbance of the spray at the right-hand front edge of the plate seen in figures 19 and 20 is attributable to the plate attachment.

Figure 20: flat glass plate as in figure (19), but with $\beta = 25°$, taken diagonally from the rear. Because the spray thickness (for equal proportion of spray drag to total drag increases with the square of the speed, the spray formation is considerable. The contour of the plate and particularly its nonvisible part were added later. The forward edge of the pressure surface is covered by the spray; it is located at about the same place as in figure 19.

Figure 21: V-bottom glass plate, 20 centimeter in width, angle of dead rise: $180° - 2.20° = 140°$; $\beta \sim 10°$; other particulars as those of figure 19. Clearly visible is front edge of pressure surface (running diagonally backward from the keel) and the forward lateral edge of the spray under the glass plate (almost crosswise to the spray): the asymmetry is probably due to an inclination of the water surface following a wave. The part of the spray forming the forward lateral edge is very thin and is immediately blown backward by the slipstream on leaving the protecting bottom surface, while the part of the spray emerging farther back from the forward edge of the pressure surface maintains its direction longer because it is thicker.

As a continuation of the forward edge of the pressure surface on each side toward the back a bright curved line is visible. Along this line a scarcely discernible plume emerges from the free surface which in figure 22 forms a plainly visible blister. The inclination of this blister along its point of origin is fairly great, considerably greater than the angle of dead rise. Its slight lateral extent points to its low absolute speed as proved by test. Theoretically it can be readily proved that such a blister cannot form on flat bottoms.

Figure 22: on this V-bottom (as in fig. 21) the spray forming at the forward edge of the pressure surface is comparatively flat, while farther back the steeper plume coming from the free surface forms the blister.

Figure 23: V-bottom plate as in figure 21 photographed diagonally from the rear.

APPENDIX

CORRELATED MATHEMATICAL RESULTS FOR THE ANALYZED LIMITING CASES

NOTATION

R resultant force on the planing surface

A lift

W total drag

W_s spray drag

W_i induced drag (due to finite planing surface width) for gravity-free motion

W_g gravity drag (wave drag) for planing surface of infinite width

M moment of planing force about the trailing edge of the planing surface

b width of planing surface

l average length of pressure surface = area of pressure surface divided by b

f deflection of curved planing surface, measured over the chord of length l

β angle of attack; for curved planing surfaces; angle of attack of the chord of length l

β_w "effective" angle of attack = β minus angle of downwash β_i or β_g

β_i angle of downwash due to finite width of planing surface in gravity-free motion

β_g angle of downwash due to gravity for planing surface of infinite width

V planing speed

ρ density of fluid

L wave length

x auxiliary quantity; to be taken from figure 18

Plate of Infinite Width; Gravity-Free Motion

Flat Plate, Finite Angle of Attack

$$R = x \frac{\pi}{2} \rho V^2 \beta_w b l \tag{10}$$

$$W_s = R \sin \beta_w \tag{11}$$

$$A = R \cos \beta_w \tag{12}$$

Flat and curved plates with infinitely small inclination:

$$R = A = \pi \rho V^2 b \left(f + \frac{1}{2} l \beta_w \right) \tag{13}$$

$$W_s = \frac{1}{2} \pi \rho V^2 \beta_w^2 b l \tag{14}$$

$$M = \frac{1}{2} \pi \rho V^2 b l \left(f + \frac{3}{4} l \beta_w \right) \tag{15}$$

$$\delta = - \pi l \beta_w^2 = \frac{W_s}{2 \rho V^2 b} \tag{16}$$

These equations are exact with $\beta = \beta_w$ for gravity-free motion and infinite plate width; it is then $W = W_s$.

But in given form these equations are equally applicable to the following.

Finite Plate Width; Gravity-Free Motion

For plates with finite span an induced drag occurs [1] (almost independent of plate form and length):

---

[1]Equations (17) to (23) are exact only for elliptic lift distribution over the span of the plate. The differences in other cases can be computed, but are of doubtful importance for the planing problem. These equations are also exactly valid only for infinitely small β. In consequence R was substituted for A (in contrast to airfoil theory).

$$W_i = \frac{4 R^2}{\pi \rho V^2 b^2} \tag{17}$$

This equation does not hold for long plates and at the same time greater angles of attack.

For infinitely short plates equations (10) to (17) are valid with

$$\beta_w = \beta - \beta_i \text{ where } \beta_i = \frac{4 R}{\pi \rho V^2 b^2} \tag{18}$$

From equation (18) and (13), (14), (17), for example, it yields

$$R = \frac{\pi \rho V^2 b (f + 0.5 \times l \beta)}{1 + \frac{2l}{b}} \tag{19}$$

$$W_s = R \frac{\beta b - 4f}{b + 2l} \tag{20}$$

$$W_i = R \beta_i = \frac{4R^2}{\pi \rho V^2 b^2} \tag{21}$$

For any long flat plate with infinitely small β

$$A = \frac{W_i}{W} \frac{\pi}{4} \rho V^2 b^2 \beta \tag{22}$$

$$W = A\beta = W\left(\frac{W_i}{W} + \frac{W_s}{W}\right) \tag{23}$$

$\frac{W_i}{W}$ and $\frac{W_s}{W}$ in respect to plate length are read from figure 9.

Infinitely small inclination, any plate form: for stationary and nonstationary motion of any shape of planing surface with any variable shape of pressure surface, the total force R follows the vector equation

$$R = \frac{1}{2} (T - S) \tag{24}$$

T denotes the total force on the equally moving wing, whose shape and eventually variable contour is identical with that of the planing surface; S is the resultant of all suction force applied at the leading edge of this wing.

The only difficulty in solving the problem in a few cases (reference 2, secs. 10, 12, 14, 15) is the determination of the contour of the pressure area of the planing surface.

Plate of Infinite Width — Gravity Taken into Consideration

Wave length is given by the formula

$$L = \frac{2\pi V^2}{g} \tag{25}$$

The wave height a for any chosen pressure distribution follows from the relation [1]

$$\frac{\rho^2 V^4 a^2}{4} = \left(\int_0^l p \cos \frac{2\pi x}{L} \, dx \right)^2 + \left(\int_0^l p \sin \frac{2\pi x}{L} \, dx \right)^2 \tag{26}$$

x indicates the position of the several pressure lines pdx (fig. 12). From a the gravity drag (wave drag) (reference 5, p. 466, equation (3)) is

$$W_g = \frac{1}{4} g \rho a^2 b \tag{27}$$

If a pressure peak is chosen on the forward edge with a pressure distribution corresponding to figure 2 the spray drag (reference 2, equation (18)) follows from the respective spray thickness δ as

$$W_S = 2 \rho V^2 \delta b \tag{28}$$

A problem still to be solved is the clear representation of the relationship between pressure distribution and plate form for longer plates. For (infinitely) short plates equations (10) to (17) [2] are applicable with

---

[1] This relation originates with Lamb (reference 5, p. 451, equation (27)) by application of the law of superposition to the infinitely many pressure lines pdx.

[2] Equations (10), (11), and (12), should remain exact for finite β, provided β_g is infinitely small. But then it should be observed (for instance, in equation (29)) that aside from the planing force R the reactive force $2V \rho V \delta b$ corresponding to the spray, acts on the fluid. However, this consideration was not explored.

$$\beta_w = \beta - \beta_g \quad \text{where} \quad \beta_g = \frac{R_g}{\rho V^4 b} \tag{29}$$

The equations for wave height and gravity drag take the simple form of equations (6) and (7), respectively.

DISCUSSION

Dr. F. Weinig: The speaker has shown that for infinitely small angles of attack and gravity-free motion the flow on the lower surface of a planing surface is exactly comparable with that at the lower surface of an airfoil. It may be shown that this comparison remains very approximately valid for greater angles of attack also. The dependability of this comparison can be proved on the example of the flat planing surface and the submerged flat plate. Figure 1 shows the pressure distribution at the lower surface of the flat airfoil and at the flat planing surface for the area behind the stagnation point. The agreement is seen to be close up to fairly great angles of attack. This comparison needs to be supplemented for the area before the stagnation point. Since the pressure on the planing surface in this area drops asymptotically to zero – in contradistinction to the wing – the comparison requires a special consideration – the introduction of an effective length.

From the satisfactory agreement for the area behind the stagnation point for the flat plate we may infer a good agreement for the other plate forms also. In that event the pressure distribution for a planing surface of any profile and any setting could be calculated. The result for a slightly curved profile of the third order is given here.

By profile is meant the form of the planing surface between stagnation point and trailing edge, making the stagnation point the "leading edge" of the profile. The leading edge of the thus defined profile and trailing edge is to have the abscissa $x = -1$ and $x = +1$; the x-axis is to be coincident with the profile chord. The profile is to follow the equation

$$y = y_1 - y_2$$

whereby (Birnbaum, Z.f.a.M.M., 1924, p. 277)

$$y_1 = \frac{v_1}{2}(1 - x^2)$$

$$y_2 = \frac{v_2}{2}(1 - x^2)\frac{4}{3}x$$

The flow past the profile is smooth when set at

$$\nu_o = \frac{\nu_2}{3}$$

with respect to the horizontal. The velocity distribution at the profile is

$$\frac{w_o}{w_\infty} = 1 - \nu_1 \sin \lambda + \nu_2 \sin 2\lambda$$

with $\lambda = \arccos x$. Hence in this case the leading edge ($\lambda = \pi$) where $\frac{w_o}{w_\infty} = 1$, is no correct stagnation point. In general the profile must be set at a greater angle. Let $\delta = a - \nu_o$ be the setting with respect to the direction ν_o.

On the pressure side of the profile (cf. F. Weinig, W.R.H. 1931, p. 115):

$$\frac{w\delta}{w_o} = \cos \delta \left[1 - \sqrt{\frac{1-\xi}{1+\xi}} \tan \delta \right]$$

That is, the stagnation point lies in $\xi = -\cos 2\delta$. In our comparison $\xi = -\cos 2\delta$ is to coincide with $x = -1$ and $\xi = +1$ with $x = +1$. Hence

$$\xi = \sin^2 \delta + \cos^2 \delta \, x$$

Furthermore the velocities at the trailing edge shall be equal. In first approximation

$$\frac{w\delta}{w_o} = 1 - \sqrt{\frac{1-x}{\frac{1+\sin^2\delta}{1-\sin^2\delta} + x}} \tan \delta$$

hence

$$\frac{w\delta}{w_o} = \left[1 - \nu_1 \sin \lambda + \nu_2 \sin 2\lambda \right] \left[1 - \sqrt{\frac{1-x}{\frac{1+\sin^2\delta}{1-\sin^2\delta} + x}} + \tan \delta \right]$$

must therefore be valid for the planing surface profile. The pressure distribution p, since all ν_1 shall be small is reproduced by

$$\frac{p}{q} = 1 - \left[1 - 2\,\nu_1 \sin\lambda + 2\nu_2 \sin 2\lambda\right]\left[1 - \sqrt{\frac{1-x}{\frac{1+\sin^2\delta}{1-\sin^2\delta}+x}}\tan\delta\right]^2$$

As found by integration the lift coefficient in first approximation is

$$\xi_a = \pi \sin\left(\delta + \frac{\nu_1}{2}\right)\left(1 - \frac{\pi}{2}\left(\delta + \frac{\nu_1}{2}\right)\right)$$

The formula for $\frac{p}{q}$ still gives satisfactory results for a part before the stagnation point when putting $\lambda = \pi$ for this part and using the formula only up to where $\frac{p}{q} = 0$. Subsequently this part is then visualized to be $\sim$ three times enlarged. Observe also the water surface behind the planing surface (fig. 2). By means of the pressure point theory a wave pattern behind the planing surface can be secured for the two-dimensional flow. Now, while agreement is to be expected for small Freude numbers, Barillon has reported that such agreement occurs only directly behind the planing surface. Only higher speeds are considered. This results in a flow process known in hydraulics as backwash (cf. Barillon, Hydrom. Probl. d. Schiffs, p. 139).

The backwash behind a planing surface, the backwash behind a sluice discharge and the smacking together of the water behind a cavitation zone (fig. 3) have great similarity. For the position of the backwash the form of the flow obstacle is obviously of little importance. The controlling factor, aside from the thickness b of the obstacle, evidently is the ratio $R^{1/2}$ of the speed at the trailing edge to the undisturbed speed at some distance: $R^{1/2} = \frac{w_{max}}{w_\infty}$. The speed w_{max} at the trailing edge of a planing surface is a little higher than that at the surface of the water near the leading edge w_∞. Let l' be the wetted length, α the angle of attack. The trailing edge then lies by $h = l' \sin\alpha$ deeper than the leading edge. With $H = \frac{1}{2g} w^2_\infty$ then

$$w_{max} = \sqrt{2g\,(H + h)}$$

whence

$$R = 1 + \frac{l' \sin \alpha}{H}$$

With b as the thickness of the flow obstacle the length of the cavitation zone was found (cf. Weinig, Hydrom. Probl. d. Sch. p. 294, or W.R.H. 1932, p. 255) at

$$\frac{L}{b} = \frac{2}{R-1}$$

For the analogy of the planing surface b must be put = $2l' \sin \alpha$. Then

$$\frac{L}{2\, l' \sin \alpha} = \frac{2}{\frac{l' \sin \alpha}{H}}$$

or

$$\frac{L}{H} = 4$$

The position of the backwash on the planing surface is therefore independent of the angle of attack as long as the flow can be regarded as two-dimensional For finite width B of planing surface a relationship with aspect ratio $\frac{l' \sin \alpha}{B}$ is additive. Wave trains leave from both ends of the trailing edge which approach each other more and more (cf. Sottorf, Experiments with Planing Surfaces, Part IV, appears shortly in W.R.H.). When these waves meet the water sprays high in the air, resembling a fountain (roach). The analogy of this fountain is, the backwash. For the location of this roach

$$\frac{L}{H} = f\left(\frac{l' \sin \alpha}{B}\right)$$

must be valid. By the quantity B is understood, as the interpretation (figure 5) (0) of Sottorf's tests manifests,

$$L = l' + a$$

where a is the distance of this fountain from the trailing edge of the planing surface.

No difference is made in the derivations between $2\, l' \sin \alpha$ and B. Therefore, if the premises are admissible, it should

$$\frac{L}{H}\left(\frac{2\, l' \sin \alpha}{B}\right) \sim \frac{L}{H}\left(\frac{B}{2\, l' \sin \alpha}\right)$$

The interpretation of the tests indicates (fig. 5, o) that this even still holds true to some extent.

In Sottorf's tests the values of α, l' and a were determined. The tests were made at $w_\infty = 6$ meters per second speed and with six different planing surface widths $B = 0.15 \div 0.6$ meter. The loading was 18 kilograms.

Dr. G. Weinblum: Naturally other possibilities of identification in earlier reports fell victims to the mathematically difficult explanation of the gravity effect... Professor Wagner contrived to escape the afore-mentioned difficulties and has presented to us the results of a planing theory with which – in the vernacular of the speaker – something can be done.

As concerns the pressure point theory a definite advance has been achieved – the inclusion of the planing drag for prescribed bottom forms.

The introduction of the spray concept is opportune and well founded in principle; this portion of the fluid motion could naturally be also regarded as a part of the wave process as the pressure point theory does; but there would not be much gained by it, because at deflection of the spray jet the pattern of an infinitely small wave inclination which hydrodynamics uses as basis of its considerations, forms no practical approximation.

As voiced by the chairman, the utilization of the airfoil theory is an important advance of the planing problem. Horn was probably the first to point out such an analogy of the processes in his ship theory. In the past the use of the term induced drag was regarded as fictitious, the consideration of wave drag was preferred but Wagner's theory justifies Horn's conception.

H. Wagner's Reply: "Concerning the remarks by Dr. Weinig on backwash, etc. I am unable to reply within this brief period. I was gratified to hear that Dr. Weinig has already concerned himself with my previously published report and is able to indicate new developments. I have limited myself in this airfoil comparison to the case for which I could show exact agreement; this is the case of so small angles of attack that in the principal area the force on upper and lower surface is the same. Dr. Weinig suggested an improvement of the comparison (for the case of stationary motion) by referring it on the wing solely to the lower surface and I would like to concur in his view that by this means a closer agreement for greater angles of attack can be achieved.

I wish to thank Dr. Weinblum for his friendly exposition. I fully agree with him. As to his remark about Dr. Horn I would like to point out that Dr. Horn, at least as regards the resistance, has alluded to a comparison with the airfoil. But he did not carry through this

comparison because in the absence of the knowledge of the spray drag an accurate comparison was impossible."

Translation by J. Vanier,
National Advisory Committee
for Aeronautics.

REFERENCES

1. Horn: Handbuch der physikalischen und technischen Mechanik, Bd. 5, 1928, secs. 75, 76, 77.

Schröder, Paul: Z.F.M., Jan. 1931.

Wagner, H.: Z.F.M., Jan. 1931.

2. Wagner, H.: Über Stoss- und Gleitvorgänge an der Oberfläche von Flüssigkeiten. Z.f.a.M.M., Aug. 1932.

3. Glauert, B.: Die Grundlagen der Tragflügel und Luftschraubentheorie, deutsch von Holl. Julius Springer (Berlin), 1929, p. 111.

4. Blenk, Hermann: Der Eindecker als tragende Wirbelfläche. Z.f.a.M.M., Feb. 1925, pp. 36-47.

5. Lamb, Horace: Hydrodynamics. Cambridge Univ. Press, 1931.

6. Sottorf, W.: Experiments with Planing Surfaces. NACA TM No. 661, 1932.

. Weinblum: Über Berechnung des Wellenwiderstandes usw. Z.f.a.M.M. 1930, p. 453.

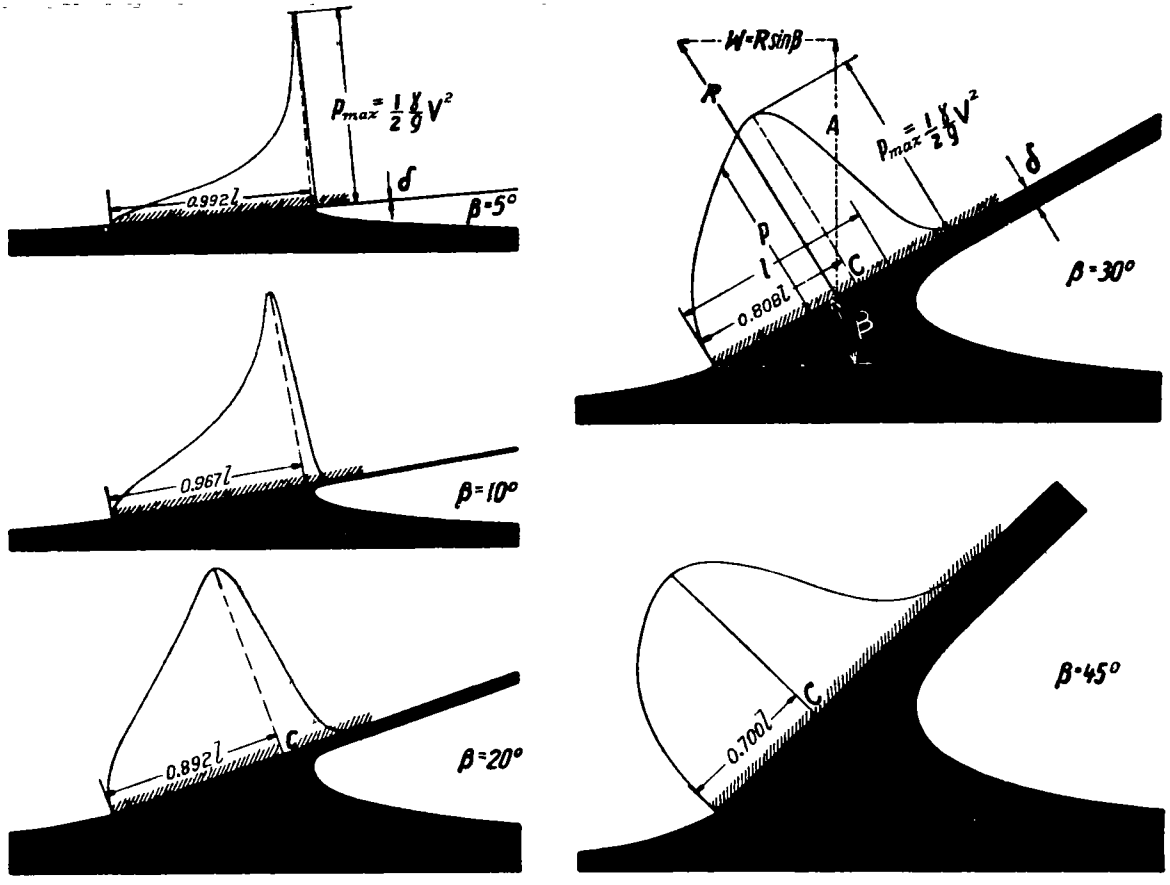

Figure 1.— Surface of fluid and pressure distribution for flat plates of infinite width in gravity-free motion. For plates of finite width angle β would be replaced by β_w according to equation (18); for short plates of infinite width under gravity effect angle β is replaced by β_w according to equation (29).

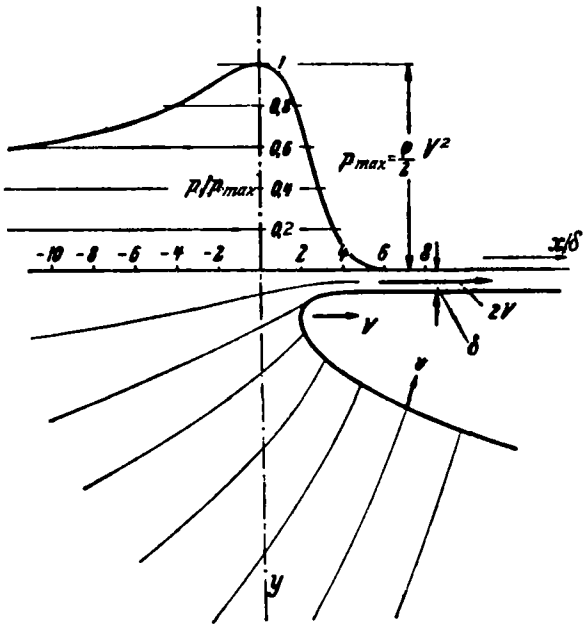

Figure 2.– Pressure distribution p over the plate and flow in the area of the spray root. The streamlines shown are those for moving plate and static fluid at infinity.

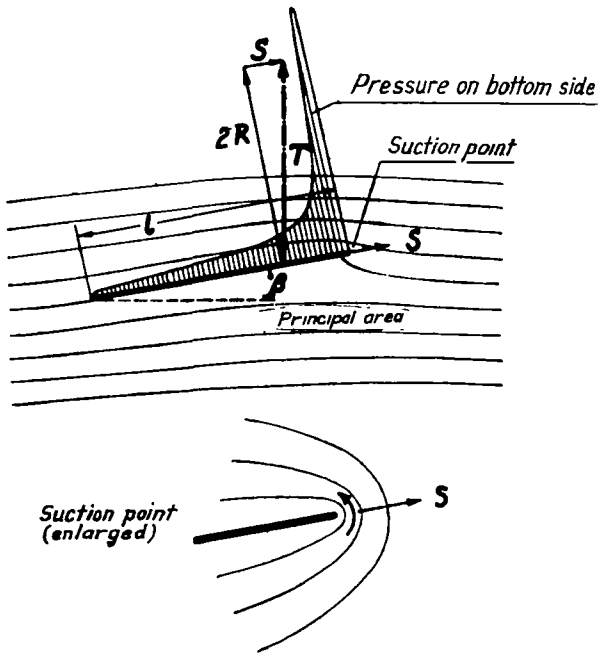

Figure 3.– Flat airfoil of infinite span and infinitely small angle of attack β; suction point.

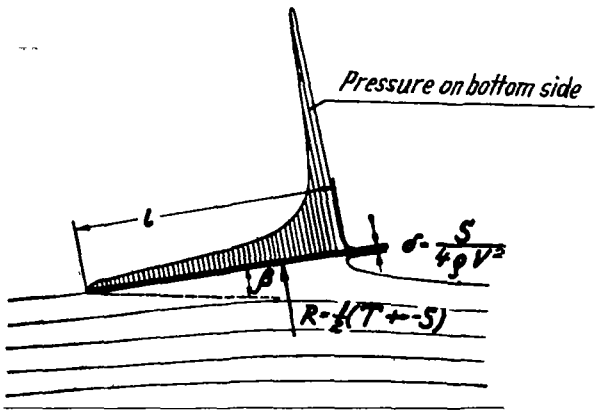

Figure 4.– Flat planing surface of infinite width with infinitely small angle β.

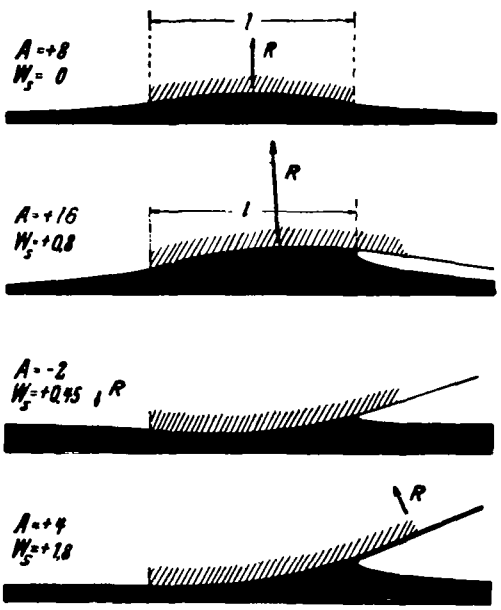

Figure 5.– Surface of fluid and forces on several circular curved planing surfaces of infinite width; the forces are comparatively to scale.

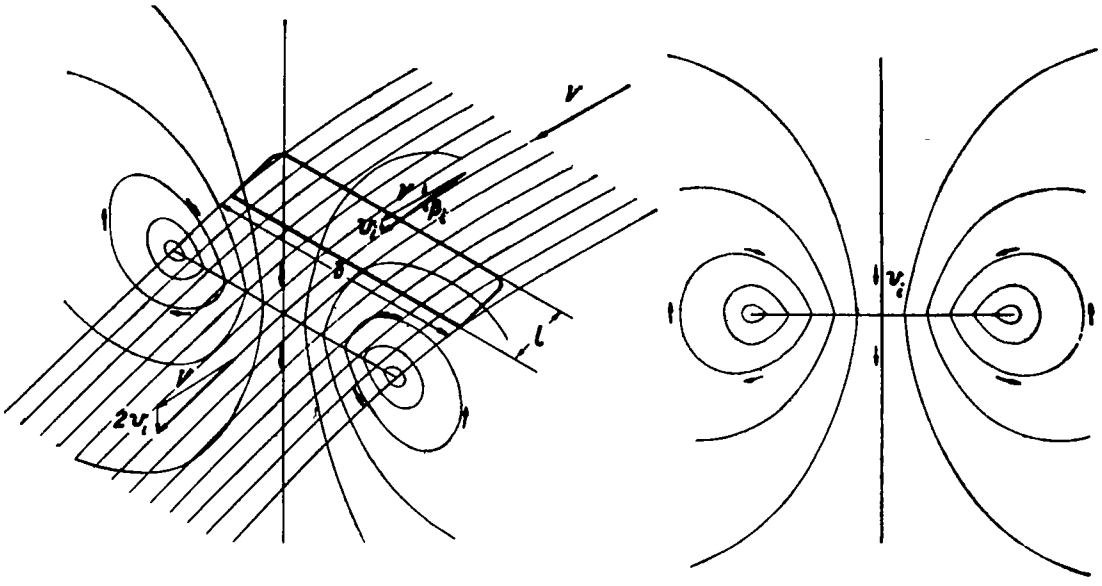

Figure 6.– Prandtl's airfoil theory; the wing of finite span is in comparison to the wing of infinite span – in a downwardly directed curved flow.

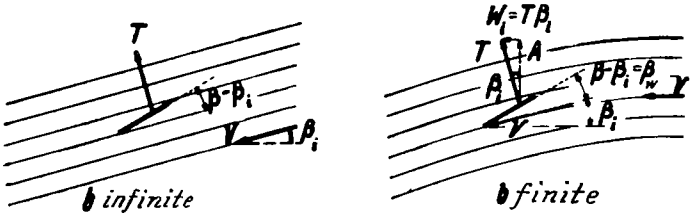

Figure 7.– Comparison of forces at a wing of finite and infinite span.

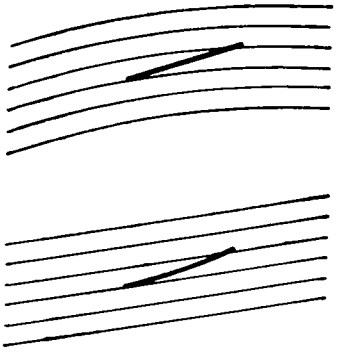

Figure 8.– The behavior of a flat airfoil in curved flow (top picture) is identical with that of a cambered airfoil in level flow (bottom picture).

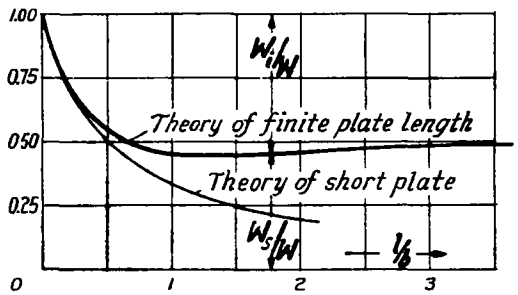

Figure 9.– Contribution of induced drag W_i and spray resistance W_s to the total drag W on flat plates of different aspect ratio l/b. The theory of finite plate length and reliable airfoil tests include only plate lengths of $0 \leqq l \leqq b$. Accordingly the curve beyond $l/b = 1$ was approximately lengthened up to the theoretically acceptable value 0.5 for plates of infinite length (cf. reference 2, p. 205).

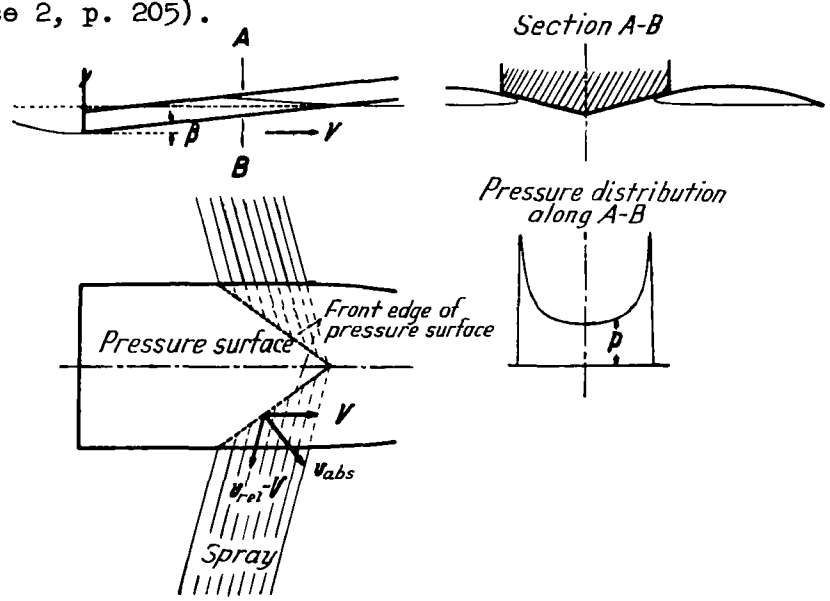

Figure 10.– Processes during planing of V-bottom boat – $v_{rel} = V$ is the speed of the spray relative to the planing boat; $r_{abs} = v_{rel}$ is the absolute speed of the spray.

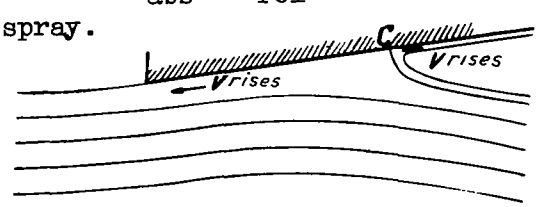

Figure 11.– The speed rises in direction of the speed. In consequence of which the friction has no substantially modified effect – no form drag.

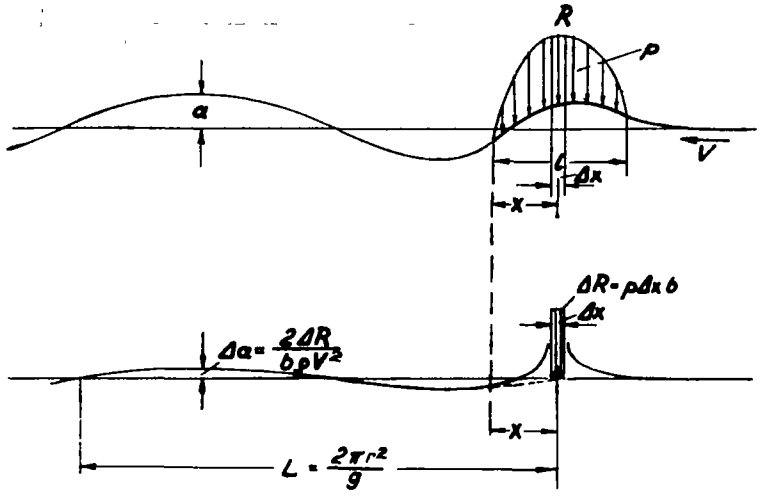

Figure 12.– Division of a pressure surface (two-dimensional problem) in pressure lines.

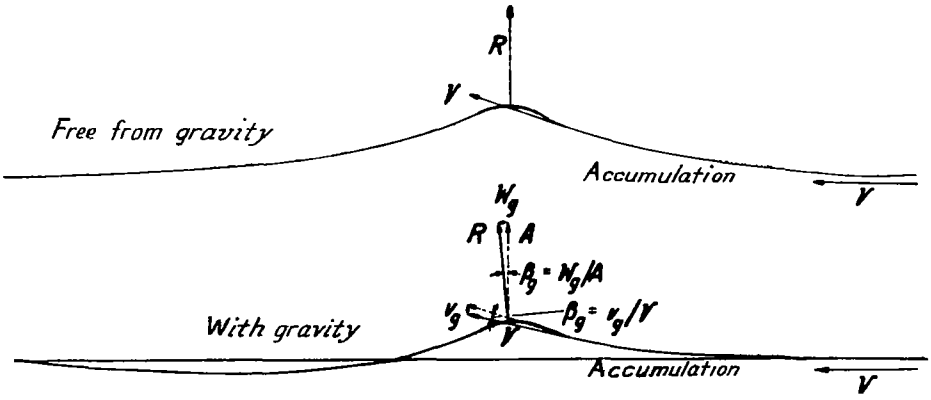

Figure 13.– The gravity effects a sinking of the impact area and as a result thereof a rotation of the flow picture and the introduction of a "gravity resistance."

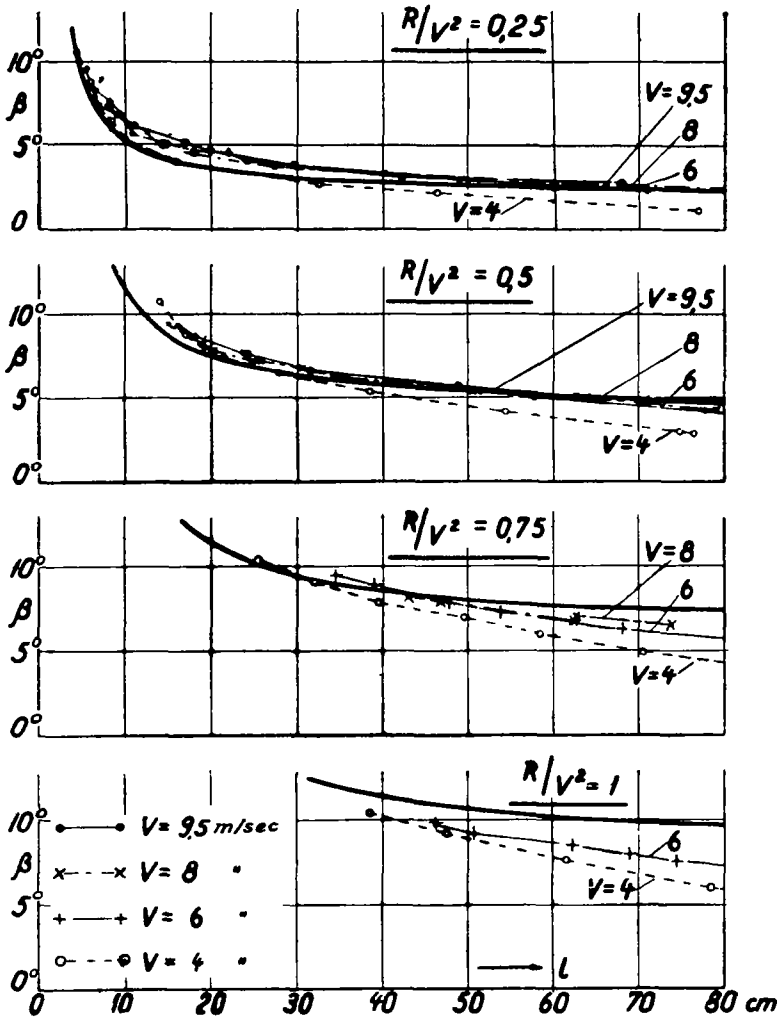

Figure 14.– Flat plates of 30 cm is width compared by theory and test; the four plots correspond to the load groups I to IV of Sottorf's tests. The theoretical values were computed by equation (10) with β_w according to equation (18). Sottorf's test data were reduced to forces at right angles to the plate.

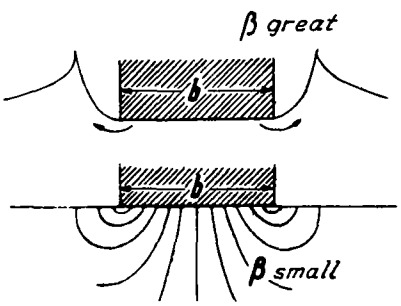

Figure 15.– The tests indicate that at greater β, hence also at greater depths of immersion, a wider portion of the fluid is involved.

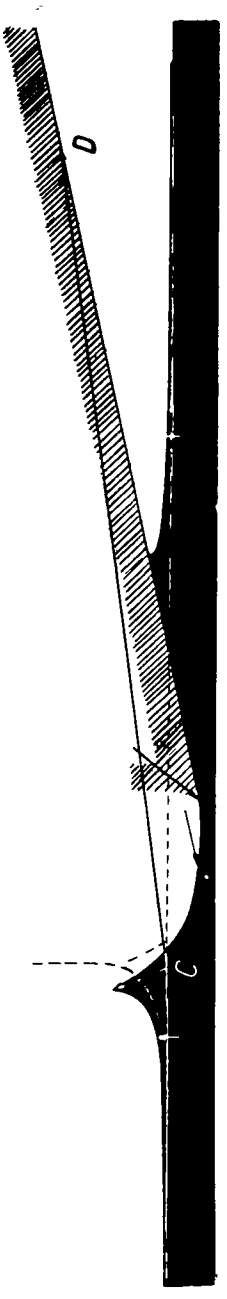

Figure 16.- Setting on a slip, the arrows indicate the speed for several points of the surface.

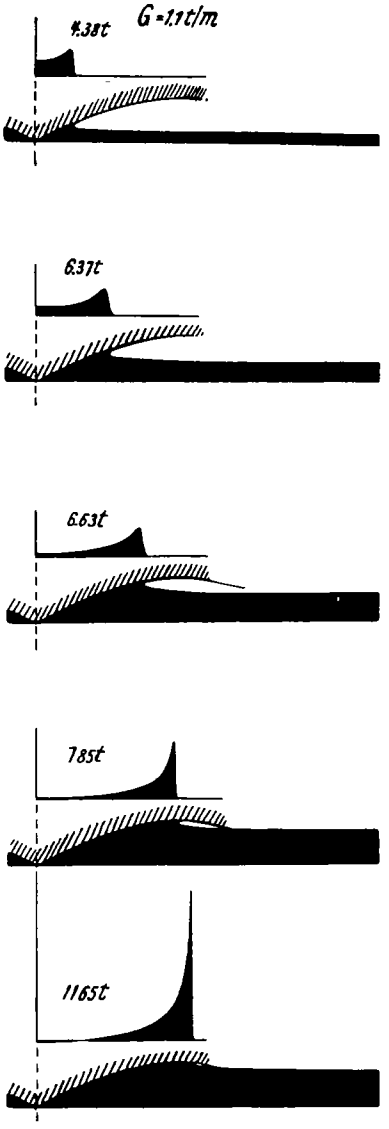

Figure 17.- Impact of a long V-bottom boat of 2 m total beam, 1100 Kg. per m length in weight with an initial rate of impact of 5 m/sec. The figures are the impact forces in tons per meter of length.

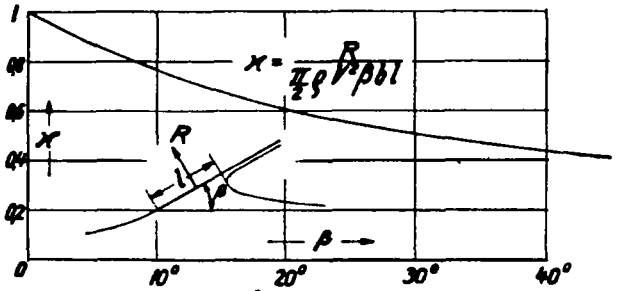

Figure 18.– Diagram for predicting the mathematical quantity x. For plates of finite width and for gravity-affected motion β must be visualized replaced by β_w.

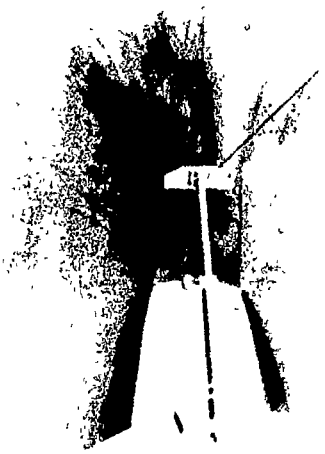

Figure 19

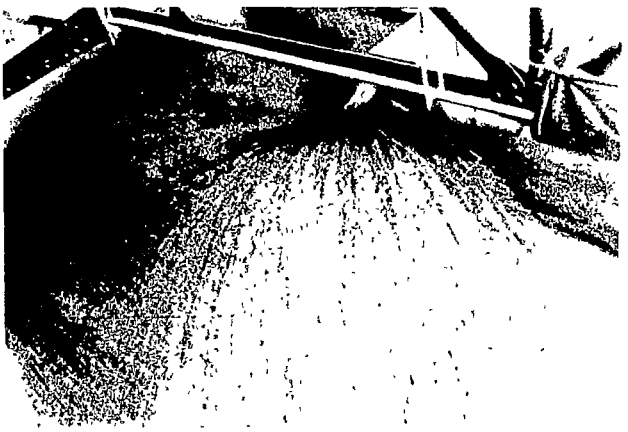

Figure 20

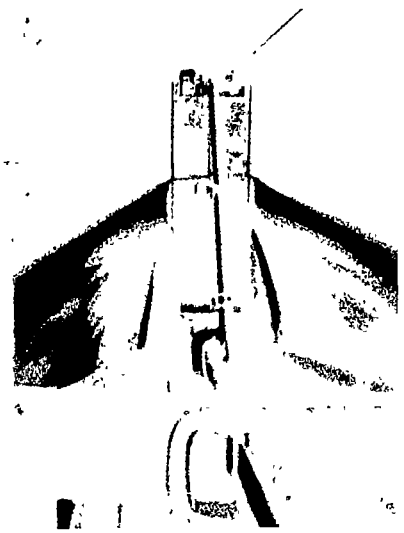

Figure 21

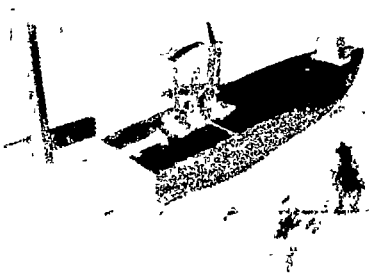

Figure 22

Figure 23

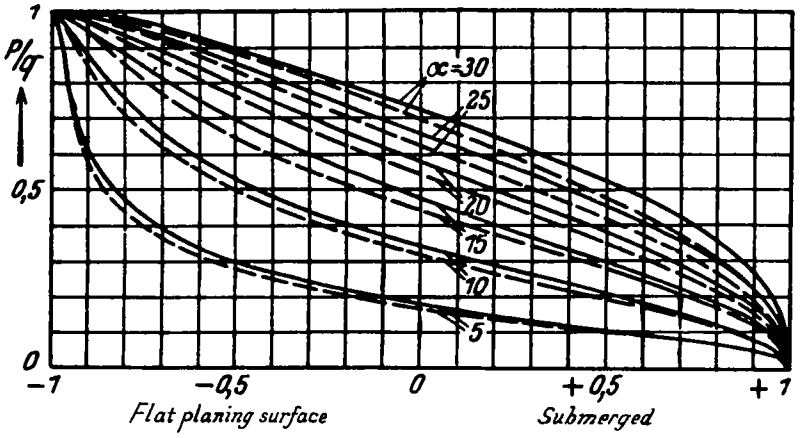

Figure 24.– Pressure distribution at lower surface of the flat airfoil and at the lower surface of a flat planing surface for the area behind the stagnation point.

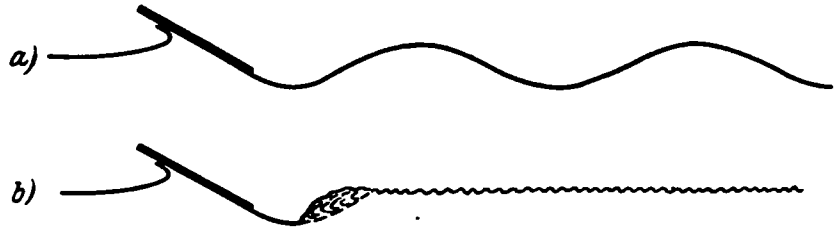

Figure 25.– Surface of water behind the planing surface.
(a) at formation of waves
(b) at formation of backwash

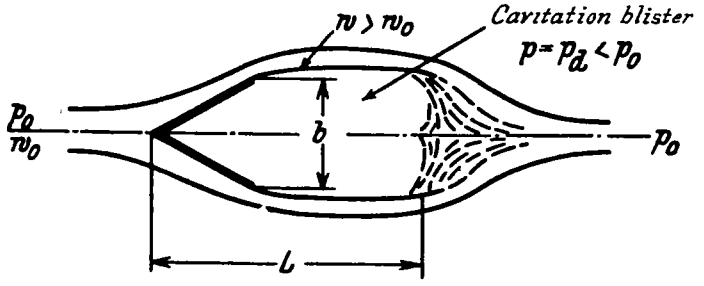

Figure 26.– Flow past a submerged obstacle with cavitation.

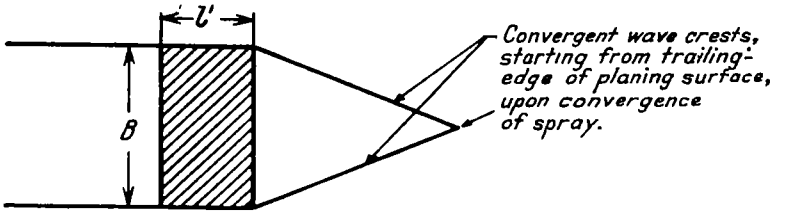

Figure 27.– Flow behind a planing surface of infinite width.

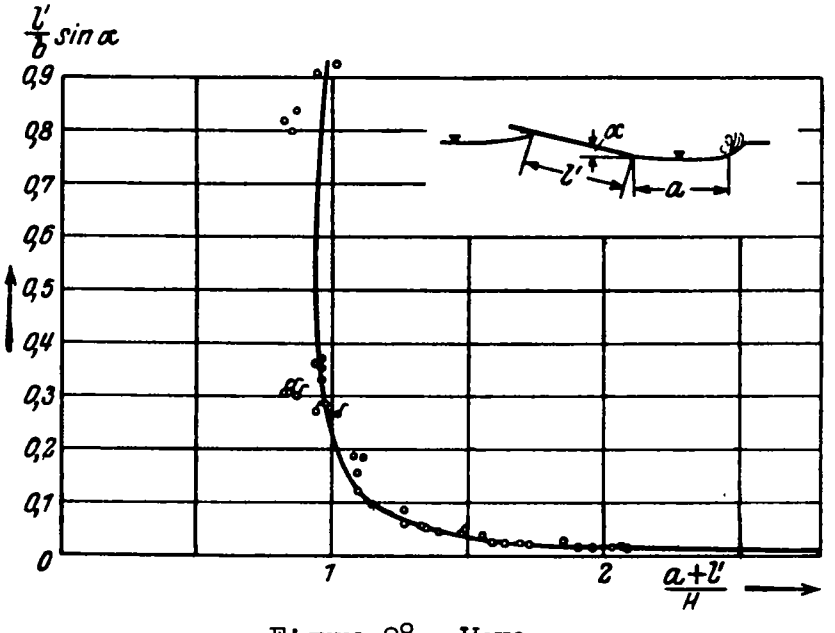

Figure 28.– Wave.